ELSEVIER

Palaeogeography, Palaeoclimatology, Palaeoecology 203 (2004) 73–93

PALAEO

www.elsevier.com/locate/palaeo

Contrasting glacial/interglacial regimes in the western Arctic Ocean as exemplified by a sedimentary record from the Mendeleev Ridge

Leonid Polyak [a,*], William B. Curry [b], Dennis A. Darby [c], Jens Bischof [c], Thomas M. Cronin [d]

[a] *Byrd Polar Research Center, Ohio State University, Columbus, OH 43210, USA*
[b] *Woods Hole Oceanographic Institution, Woods Hole, MA 02543, USA*
[c] *Old Dominion University, Norfolk, VA 23529, USA*
[d] *US Geological Survey, Reston, VA 20191, USA*

Received 1 August 2002; received in revised form 14 August 2003; accepted 19 September 2003

Abstract

Distinct cyclicity in lithology and microfaunal distribution in sediment cores from the Mendeleev Ridge in the western Arctic Ocean (water depths ca. 1.5 km) reflects contrasting glacial/interglacial sedimentary patterns. We conclude that during major glaciations extremely thick pack ice or ice shelves covered the western Arctic Ocean and its circulation was restricted in comparison with interglacial, modern-type conditions. Glacier collapse events are marked in sediment cores by increased contents of ice-rafted debris, notably by spikes of detrital carbonates and iron oxide grains from the Canadian Arctic Archipelago. Composition of foraminiferal calcite $\delta^{18}O$ and $\delta^{13}C$ also shows strong cyclicity indicating changes in freshwater balance and/or ventilation rates of the Arctic Ocean. Light stable isotopic spikes characterize deglacial events such as the last deglaciation at ca. 12 ^{14}C kyr BP. The prolonged period with low $\delta^{18}O$ and $\delta^{13}C$ values and elevated contents of iron oxide grains from the Canadian Archipelago in the lower part of the Mendeleev Ridge record is interpreted to signify the pooling of freshwater in the Amerasia Basin, possibly in relation to an extended glaciation in arctic North America. Unique benthic foraminiferal events provide a means for an independent stratigraphic correlation of sedimentary records from the Mendeleev Ridge and other mid-depth locations throughout the Arctic Ocean such as the Northwind and Lomonosov Ridges. This correlation demonstrates the disparity of existing age models and underscores the need to establish a definitive chronostratigraphy for Arctic Ocean sediments.
© 2003 Elsevier B.V. All rights reserved.

Keywords: Arctic Ocean; Quaternary; stratigraphy; paleoceanography; glaciation; ice rafting; Foraminifera; Ostracoda; stable isotopes; provenance

1. Introduction

The Arctic Ocean plays a major role in the late Cenozoic evolution of the Earth's environmental

* Corresponding author. Tel.: +1-614-292-2602; Fax: +1-614-292-4697.
E-mail address: polyak.1@osu.edu (L. Polyak).

0031-0182/03/$ – see front matter © 2003 Elsevier B.V. All rights reserved.
doi:10.1016/S0031-0182(03)00661-8

system, including the modern climatic change (e.g., Aagard et al., 1999). The most important aspects of the interaction between the Arctic Ocean and the global climate are (1) vast ice cover that increases albedo and controls a significant part of the global energy balance, and (2) the control on the oceanic thermohaline circulation through the water exchange with the Atlantic and Pacific oceans (Delworth et al., 1997; Smith et al., 2002). The Quaternary history of the Arctic Ocean features multiple dramatic changes associated with glaciations and deglaciations of the arctic periphery and sea level fluctuations. During glacial periods and low sea levels, extensive areas of shallow arctic shelves were exposed and partially covered by ice sheets, which drastically reduced the circulation within the Arctic Ocean and the inter-oceanic water exchange. This, together with more severe ice conditions in the ocean interior, had a dramatic effect on sedimentary environments. Despite the importance of the Arctic Ocean sedimentary archives for understanding the Earth's Quaternary climatic evolution, relatively few sedimentary records have become available for detailed investigation because of operational constraints in the ice-bound Arctic Ocean interior. In addition to logistical problems of obtaining sediment cores, it is difficult to develop an unequivocal stratigraphy of late Cenozoic sediments because of the meagerness of biotic remains, low sedimentation rates of mostly below 1 cm/kyr, and the unique history of the Arctic Ocean. In recent years, several late Cenozoic sedimentary records with a moderate temporal resolution have been investigated from the Arctic Ocean interior, mainly from intermediate water depths, such as on the Northwind and Lomonosov Ridges (Fig. 1; Poore et al., 1993, 1994; Phillips and Grantz, 1997; Spielhagen et al., 1997; Jakobsson et al., 2000, 2001). However, different stratigraphic approaches employed in these studies result in differing age models and contrasting

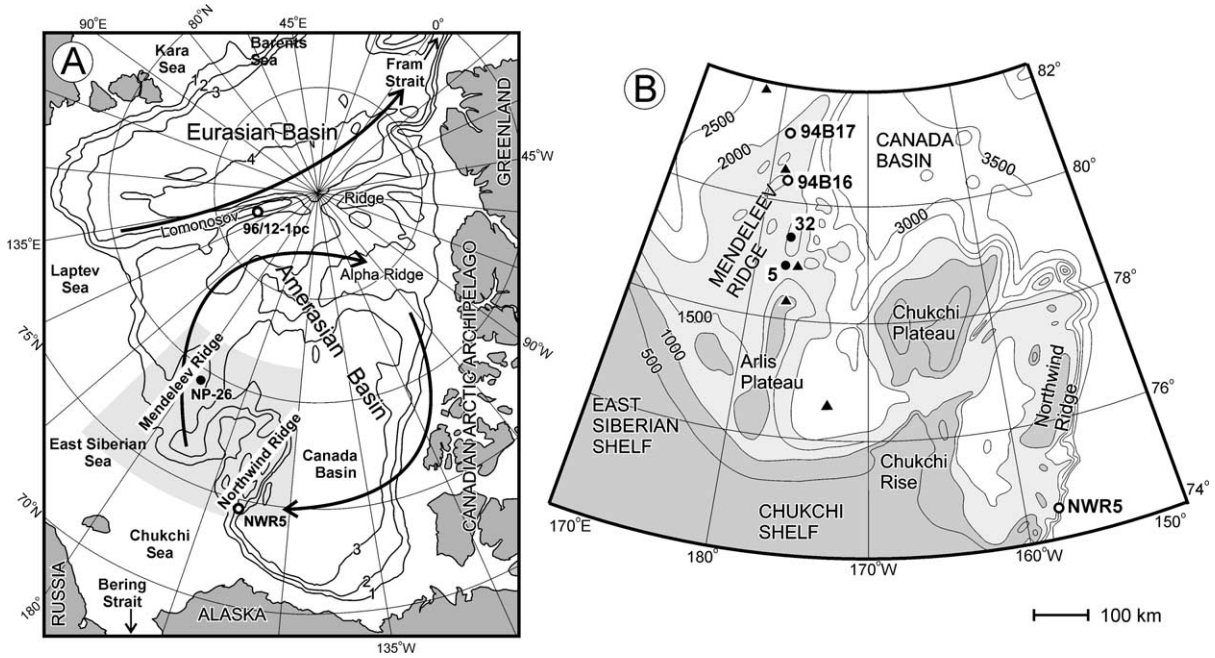

Fig. 1. (A) Map of the Arctic Ocean with bathymetry in 1-km contour lines. Inset area (B) is shaded. Black circle shows the location of NP26 cores; unfilled circles show locations of cores from Northwind and Lomonosov Ridges used for stratigraphic correlation (Fig. 10). Arrows show major current systems: Beaufort Gyre and Transpolar Drift. (B) Map of the Mendeleev Ridge and Chukchi Borderland with bathymetry in 500-m contour lines (from Perry and Fleming, 1986). Black circles show location of NP26 cores 5 and 32; unfilled circles indicate other cores referred to in the paper; triangles indicate hydrographic profiles shown in Fig. 2.

paleoceanographic interpretations. This underscores the necessity to investigate more sedimentary records from the Arctic Ocean aiming at multi-proxy studies of seafloor areas with relatively high sedimentation rates. In this paper, we present results of a multi-proxy investigation of a sediment core record from intermediate water depths at the Mendeleev Ridge in the western part of the Arctic Ocean (Amerasia Basin).

2. Study area

Mendeleev Ridge is an elevated portion of the Arctic Ocean floor extending from the East Siberian shelf towards the North Pole (Fig. 1). On the shallow southern part of the Mendeleev Ridge and adjacent Chukchi Borderland (Chukchi Plateau and Northwind Ridge), sedimentation rates are higher than in the interior of the Amerasia Basin (Poore et al., 1993; Phillips and Grantz, 1997), probably because of sediment transport from the adjacent shelves and more frequent summer ice melt. Modern sedimentation rates were estimated to be as low as 0.2–0.3 mm/kyr throughout the Amerasia Basin by ^{230}Th and pore water chemistry methods (Cranston, 1997; Huh et al., 1997); however, ^{14}C data from the Chukchi Borderland show up to two orders of magnitude higher sedimentation rates during the deglaciation and the Holocene (Darby et al., 1997).

The stratified water mass structure of the Arctic Ocean includes the low-salinity surface water, several intermediate water layers, and the bottom waters (Aagard et al., 1985). Cold and saline bottom waters are formed by the exchange with the Norwegian-Greenland Sea via the Fram Strait and by cascading of dense water ejected by ice formation on the shelves. The Amerasia and Eurasia Basins of the Arctic Ocean are separated by the Lomonosov Ridge with a sill depth of ca. 1500 m; as a result, their deep waters have somewhat differing thermohaline properties and residence times. The deep water of the Amerasia Basin is relatively warm (−0.5°C) and may have a notably old age of almost 1000 years (Macdonald and Carmack, 1991). The major intermediate water layer with a core at depths of ca. 200–500 m originates from the North Atlantic Drift; this water retains fairly high heat content resulting in temperatures >0°C throughout the Arctic Ocean (Fig. 2). The water column above this Atlantic-derived layer contains the Pacific water that inflows via the Bering Strait and is characterized by high nutrient contents and relatively low salinity of <33 psu. The balance of Atlantic and Pacific waters flowing into the Arctic Ocean varies with time (Carmack et al., 1997; Steele and Boyd, 1998). Currently, the front between Atlantic and Pacific components in subsurface waters is located along the Mendeleev Ridge (Jones et al., 1998), which underscores the significance of this area for studying the long-term changes in the Arctic circulation. The surface water of the Arctic Ocean receives the voluminous river runoff that keeps the salinity low and thus maintains the sea ice cover. Ice and the surficial waters are involved in a wind-driven circulation which forms the anticyclonic Beaufort Gyre over the Amerasia Basin (Fig. 1). The major gateway for outflowing low-salinity surface water is the Fram Strait; addition-

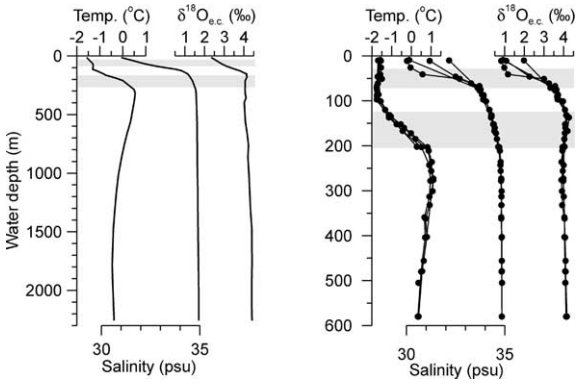

Fig. 2. Hydrographic profiles from the Mendeleev Ridge area (Fig. 1; data from Ekwurzel et al., 2001). Shown are potential temperature, salinity, and equilibrium calcite δ^{18}O (vs. PDB) estimated from temperature and water δ^{18}O using the equation of Shackleton (1974). Halocline and thermocline levels are highlighted. Right panel shows details of the upper portion of the water column. Gradient in surface salinity and δ^{18}O reflects the contribution of runoff related to the distance from the shelf.

Table 1
Geographic position of sediment cores under study

Core No.	Latitude (°N)	Longitude (°W)	Water depth (m)
NP26-5	78°58.7′	178°09′	1435
NP26-32	79°19.4′	178°04′	1610

ally, substantial volumes leave via the straits of the Canadian Archipelago and the Barents Sea.

Due to perennial sea ice cover, the productivity in the central Arctic Ocean is low, although recent studies estimate the amount of primary production as high as 15 g C/m^2/yr, much higher than previously believed (Gosselin et al., 1997). Benthic population densities appear to be higher at shallower depths, possibly due to lateral advection of food from shelves (Clough et al., 1997). Biological production in the Arctic has undergone large temporal variations, being greatly reduced during glacial periods, but possibly somewhat enhanced during the episodes of climatic amelioration, such as the early Holocene (Cronin et al., 1995).

3. Materials and methods

Sediment cores used in this study were collected with a gravity corer in 1983 from a Russian drifting ice camp 'Severnyj Polyus (North Pole) 26' (further referred to as NP26). All cores were split and described at VNII Okeangeologia, Russia (Yashin, 1985). Two closely located cores, 5 and 32, from intermediate water depths of around 1.5 km (Table 1) were continuously sampled by Polyak at 1.5–2-cm intervals for a detailed investigation. Samples were taken so as to minimize the contamination from adjacent intervals by bioturbation. The upper part of the stratigraphically longer core 5 has been damaged; therefore, we use core 32 with a similar stratigraphy to characterize the corresponding portion of the cored sedimentary record (Fig. 3). The correlation of these two cores, originally based on the lithological overview, was verified and detailed using all lithological and microfaunal characteristics under study. Initial results of the investigation of these and adjacent NP26 cores have been reported ear-

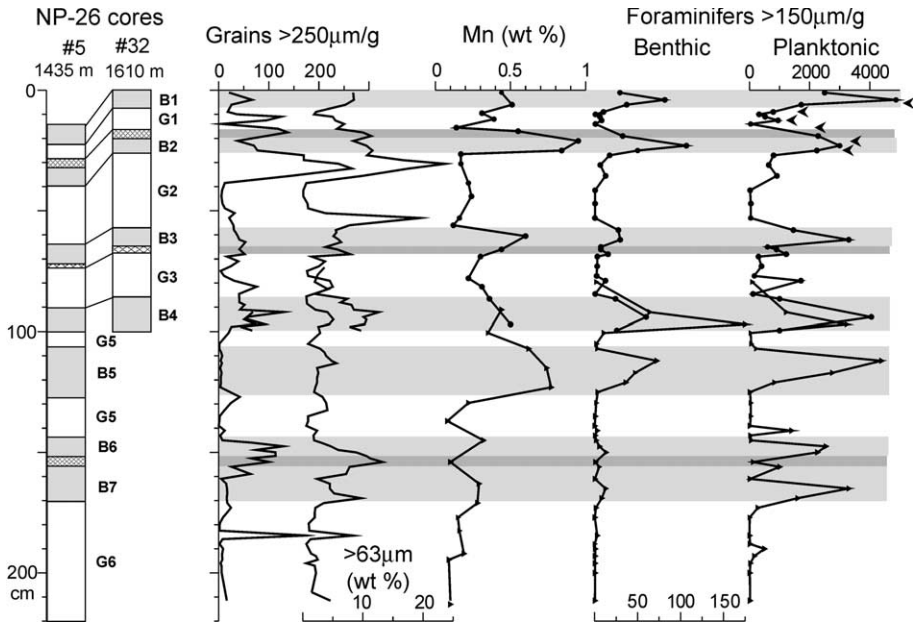

Fig. 3. Stratigraphic characterization of NP26 cores 5 and 32; core 5 is shifted 14 cm down for plotting. Indices of lithologic units (beds) used in the text are shown to the right of lithologic columns. Brown (interglacial) beds are shaded; a criss-cross pattern or darker shading shows pink-white detrital carbonate layers. Arrows next to the planktonic foraminiferal curve show position of ^{14}C ages. Manganese content was determined by XRF analysis (Yashin, 1985).

Table 2
AMS ^{14}C ages

Lab number	Depth in core (cm)	Reported age (yr BP)
AA20485	6.0	5 325 ± 105
AA35047	9.0	9 740 ± 95
AA20486	12.5	22 030 ± 580
AA35048	16.0	37 700 ± 1200
AA35049	21.0	34 000 ± 1400
AA35050	25.0	38 900 ± 1100

All age determinations were performed at the Arizona AMS Facility on tests of *Neogloboquadrina pachyderma*.

lier (Yashin, 1985; Polyak, 1986; Belyaeva and Khusid, 1990; Danilov et al., 1991). We have re-investigated the material (washed residues) from cores 5 and 32 with an emphasis on foraminiferal, ostracode, stable isotope, and clast provenance analyses. Age control for the youngest part of the record is provided by six ^{14}C ages (Table 2).

4. Results

4.1. Core stratigraphy

Sediments recovered from the Mendeleev Ridge are characterized by a distinct alternation of brown and yellowish-gray beds of 5–40 cm thickness (Fig. 3). Brown beds, which include the surficial interval, contain moderate amounts of sand and elevated concentrations of organic matter, faunal remnants, and chemical species indicative of an oxidizing environment, such as Mn and Fe^{3+} (Table 3; Fig. 3). The upper boundary of brown beds is typically distinct, whereas their lower boundary is disturbed by bioturbation. Gray beds are almost unfossiliferous and largely fine-grained, but some contain prominent sandy intervals near the top and/or bottom of gray units. We will further use a simplified lithostratigraphy, counting brown (B) and gray (G) beds from top to bottom. In addition to this cyclic lithostratigraphy, there are several thin intervals of distinctly pinkish and/or whitish coloration due to enrichment of sediment with white or pinkish-yellow carbonate clasts. A similar stratigraphy with alternating brown and gray beds and pink-white intercalations has been described for sediments from the Northwind Ridge, some 800 km southeast of the study area (Fig. 1; Phillips et al., 1992; Poore et al., 1993, 1994; Phillips and Grantz, 1997). Moreover, general patterns of the stratigraphic sequence from the Mendeleev and Northwind Ridges can be recognized throughout the entire central Arctic Ocean (e.g., Belov and Lapina, 1961; Jakobsson et al., 2000). Correlation is more tenuous with areas having extremely low sedimentation rates, such as the Alpha Ridge (Clark et al., 1980; Scott et al., 1989); still it can be maintained by means of stratigraphic markers, including pink-white carbonate layers and sandy intervals.

4.2. Microfauna

We have investigated microfauna in the size fraction >150 μm from 60 samples and 63–100 and 100–150 μm from 19 samples (Figs. 3–5). Brown beds typically contain abundant plankton-

Table 3
Characteristic lithological and geochemical features of brown and gray beds in NP26 cores from Mendeleev Ridge (from Yashin, 1985)

Feature	Brown beds	Gray beds
>100-μm sand content (%)	4.5 (0.5–14.0) [75]	3.8 (0.4–18.8) [62]
$CaCO_3$ (%)	5.3 (0.6–9.2) [26]	2.6 (0–13.2) [48]
C org. (%)	0.97 (0.56–2.10) [26]	0.69 (0.13–1.82) [48]
Soluble Fe^{3+} (%)	4.40 (3.06–5.72) [20]	3.99 (2.75–4.69) [22]
Soluble Fe^{2+} (%)	0.36 (0.14–1.07) [20]	0.84 (0.25–1.13) [22]
Mn (%)	0.39 (0.09–0.66) [16]	0.16 (0.05–0.59) [23]

Pinkish intercalations rich in carbonate clasts are not included. Notation shows mean values with minimal and maximal values in parentheses; number of analyzed samples is shown in brackets.

ic and benthic foraminifers and ostracodes, as well as occasional other faunal remains composed of calcite (echinoid spines and pteropodes) or silica (sponge spicules). In contrast, gray beds contain only scarce faunal remains that can be partially attributed to bioturbation. Planktonic foraminifers throughout the core record are represented predominantly by the only species adapted to thrive in polar latitudes, *Neogloboquadrina pachyderma* sinistral (left-coiling). In contrast, benthic faunal assemblages show significant downcore changes, superimposed on the cyclic recurrence of faunal-rich intervals. These changes show a consistent pattern in cores from various parts of the Arctic Ocean, such as the Mendeleev, Northwind, Alpha, and Lomonosov Ridges (O'Neill, 1981; Polyak, 1986; Scott et al., 1989; Belyaeva and Khusid, 1990; Poore et al., 1994; Ishman et al., 1996; Jakobsson et al., 2001), which enables long-distance correlations by means of foraminiferal and ostracode stratigraphies.

The oldest fauna recovered on the Northwind, Alpha, and Lomonosov Ridges, but not reached by NP26 cores, contains almost exclusively arenaceous foraminifers, which indicates a strong dissolution of calcareous tests (O'Neill, 1981; Scott et al., 1989; Ishman et al., 1996; Evans and Kaminski, 1998; Jakobsson et al., 2001). In contrast, calcareous foraminifers predominate in younger sediments. A marked change in calcareous benthic foraminiferal composition occurs throughout the Amerasia Basin, including NP26 cores, at the stratigraphic level of gray bed G5 (Fig. 4; Scott et al., 1989; Poore et al., 1994; Ishman et al., 1996; Jakobsson et al., 2001). Assemblages below this level are characterized by high numbers of *Bolivina arctica* in the small size fraction (63–100 μm), and relatively high content of *Cassidulina teretis* in coarser fractions. Another characteristic feature of this assemblage zone is a common occurrence of foraminifers typical for shelf areas, mostly *Elphidium* spp. Above, the assemblages are predominated by *Stetsonia horvathi* in the smaller size class and *Oridorsalis tener* in coarse fractions in cores from water depths >1 km (Poore et al., 1994; Ishman et al., 1996; Jakobsson et al., 2001); at shallower depths, the prevalent species is *C. teretis*, which thrives in the Arctic Ocean

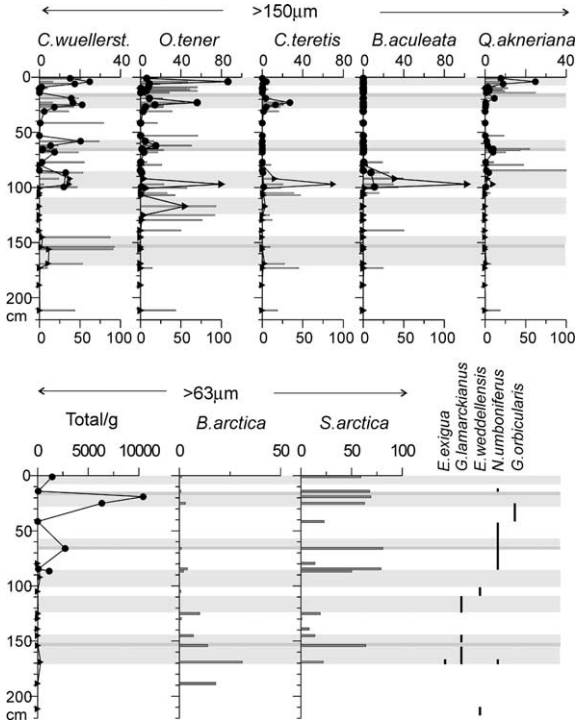

Fig. 4. Benthic foraminiferal distribution in NP26 cores (see Fig. 2 for lithology). Upper panel shows abundances per gram (curves, upper scale bars) and percentages (bars, lower scale bars) in the >150-μm size class. Lower panel shows total abundances per gram and percentages of two species in the >63-μm size class, as well as occurrence ranges of some rare species. Percentages are not shown for levels with very low abundances.

within the depth interval affected by Atlantic waters (Lagoe, 1979; Polyak, 1990; Ishman and Foley, 1996). The lower part of the *O. tener* abundance zone in cores from water depths between 1 and 2 km is characterized by the common occurrence of *Bulimina aculeata* that reaches >50% in unit B4 in the size class >100 μm (Fig. 4; Polyak, 1986; Poore et al., 1994; Ishman et al., 1996; Jakobsson et al., 2001). This species is practically absent from the Arctic Ocean today, which enables the use of its abundance spike as a distinct biostratigraphic marker.

The occurrences of some other species, notably *Epistominella exigua*, *Nuttalides umboniferus*, *Alabaminella weddellensis*, and *Gyroidinoides* spp., are also confined to certain narrow stratigraphic levels (Fig. 4) and indicate conditions unlike those in

the modern Arctic Ocean. Some of these species, such as *E. exigua*, presently inhabit the Norwegian-Greenland Sea and a limited adjacent area of the Arctic Ocean, but not the Amerasia Basin; other species, such as *N. umboniferus*, occur at present only south of the Norwegian-Greenland Sea.

The downcore distribution of ostracodes on the Mendeleev Ridge also exhibits significant changes in their composition (Fig. 5). The lower part of the sedimentary sequence with calcareous fauna (B5 to G6) contains a relatively poor, low-diversity ostracode assemblage represented by *Cytheropteron* spp. and some *Krithe glacialis* and *Polycope*. More diverse and abundant ostracodes occur upcore, in brown beds B1–B4. Among other species, this fauna consistently contains *Acetabulastoma* sp., whose life cycle is connected with sea ice (Cronin et al., 1994). A distinct assemblage dominated by *Henryhowella* sp. characterizes the transition from G2 to B2, whereas the onset of the Holocene is marked by a rise in *Cytheropteron* and *Krithe* species at the expense of *Polycope*. Although ostracodes are more scarce in the Lomonosov Ridge sediments, the general downcore change in ostracode abundance and composition there shows a pattern similar to that in NP26 cores (Jones et al., 1999; Jakobsson et al., 2001). Furthermore, the transition from the glacial/deglacial to Holocene ostracode assemblages in the Mendeleev Ridge record is similar to those described from intermediate water depths throughout the Arctic Ocean (Cronin et al., 1995).

4.3. Stable isotopes

Simultaneous measurements of $\delta^{18}O$ and $\delta^{13}C$ were run on tests of planktonic foraminifer *Neogloboquadrina pachyderma* (sin.) and two benthic species, *Cibicidoides wuellerstorfi* and *Oridorsalis tener*, believed to represent epifaunal and shallow infaunal habitats, respectively. Analyzed tests were picked from the 150–250-μm size class to minimize size-dependent effects; only some *C. wuellerstorfi* specimens were larger than 250 μm. Most *N. pachyderma* (sin.) tests had a secondary calcitic crust. Nearly all *N. pachyderma* (sin.) samples were measured twice; even more replicate analyses were performed on *C. wuellerstorfi* samples. All measurements were performed on a Finnigan MAT 252 with a 'Kiel' automated device using the standard WHOI methods (Ostermann

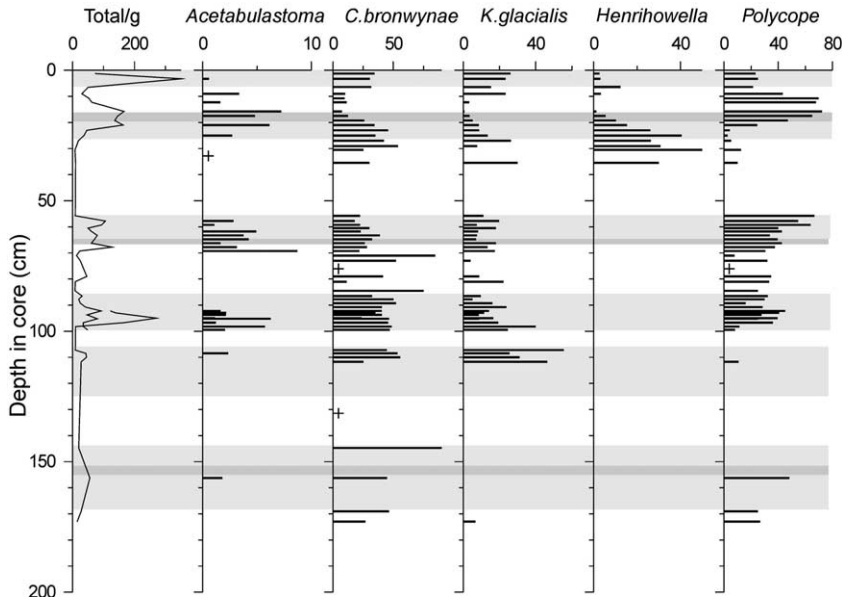

Fig. 5. Ostracode distribution in NP26 cores (see Fig. 2 for lithology). Curve on the left shows total abundances per gram in the >150 μm-size class; bars show species percentages. Crosses show presence of species in samples with very low abundances.

and Curry, 2000; www.whoi.edu/paleo/mass-spec).

Records of both planktonic $\delta^{18}O$ and $\delta^{13}C$ display pronounced cyclic variations with amplitudes often exceeding those of the global open ocean record (Fig. 6). The pattern of these variations in the youngest beds (B1–B3) is consistent with box core data from the more northern area of the Mendeleev Ridge (Fig. 1; Poore et al., 1999). Brown units are generally characterized by intermediate or high $\delta^{18}O$ values. Four distinct spikes in excess of 3‰ occur at the bottom parts of B2, B3, and B5 and immediately above B3. The low $\delta^{18}O$ spikes reaching −0.5‰ in averaged values and below −1.5‰ in individual measurements occur mostly within gray beds or at their boundaries. Below B5, $\delta^{18}O$ values are more uniform, being relatively low in both gray and brown sediments. Benthic $\delta^{18}O$ variations, especially in *Cibicidoides wuellerstorfi*, have a pattern similar to the planktonic $\delta^{18}O$ record, but with a smaller amplitude. However, some levels within G2 and at the bottom of B7 have outstanding light *C. wuellerstorfi* $\delta^{18}O$ excursions of >1‰.

The planktonic $\delta^{13}C$ record shows even more regular, cyclic variations than $\delta^{18}O$ (Fig. 6). Highest values reaching 1.5‰ characterize interglacials, whereas gray beds contain light minima of near 0‰ in averaged values and as low as under −1‰ in individual measurements. Similar to the $\delta^{18}O$ record, $\delta^{13}C$ values are relatively stable, moderately light in the oldest sediments (B6–G6); however, it is in G6 where extremely light excursions of $\delta^{13}C$ occur. Downcore changes in benthic $\delta^{13}C$ have a general pattern similar to the planktonic record, but vary in amplitudes and absolute values. *Cibicidoides wuellerstorfi* has relatively low-magnitude $\delta^{13}C$ variations, mostly below 1‰, whereas those in *Oridorsalis tener* show an amplified magnitude of 3‰ and values up to 4‰ lighter.

4.4. Provenance of ice-rafted debris (IRD)

The provenance of terrigenous sediments was studied using the petrographic composition of lithic clasts >250 μm and the chemical composition of detrital iron oxide grains (45–250 μm) de-

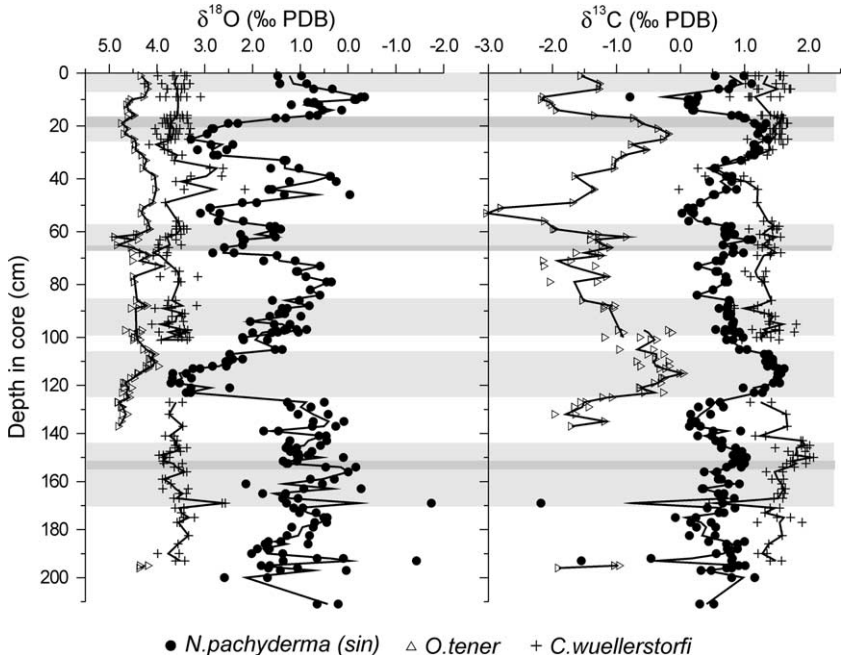

Fig. 6. Distribution of $\delta^{18}O$ and $\delta^{13}C$ in planktonic and benthic foraminifers in NP26 cores (see Fig. 2 for lithology). Symbols show individual measurements, curves show averages. $\delta^{18}O$ values in *Oridorsalis tener* are shifted +0.5‰ for plotting.

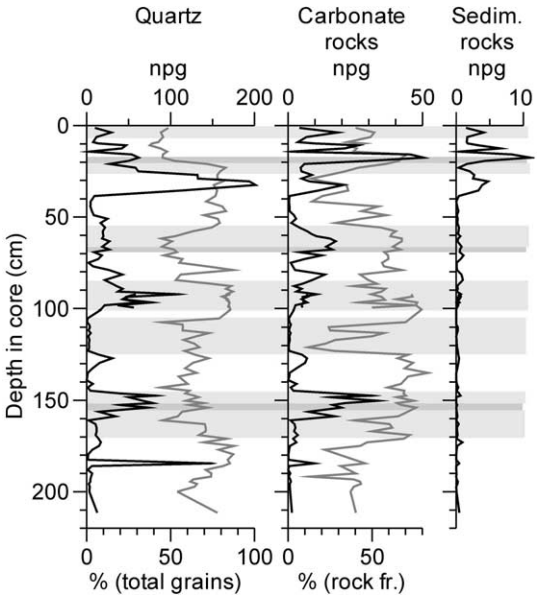

Fig. 7. Types of lithic clasts >250 μm in NP26 cores (see Fig. 2 for lithology and total clast abundance). Black curves and upper scale bars show grain number per gram (note different scales), gray curves and lower scale bars show percent of quartz in total grains and percent of carbonates in rock fragments.

termined by electron microprobe analysis (for details of methods see Darby and Bischof, 1996; Darby, 2003). These techniques have been successfully applied to the Arctic Ocean modern and Quaternary sediments by employing a large data base (300+ samples) of circum-arctic source area characterizations of shelf and coastal sediments for lithic grain type and detrital Fe oxide grain fingerprints (Bischof et al., 1996; Bischof and Darby, 1997; Darby et al., 2002). The distribution of both coarse clasts and iron oxides in the NP26 core record shows large variations indicative of changing dominant sources of sediment that is delivered to the Arctic Ocean interior by sea ice or glacier ice (Figs. 3, 7 and 8).

The unevenly distributed abundance of lithic clasts is mostly consistent with the overall sand content and features several spikes that indicate episodes of intensified sea ice rafting and/or iceberg discharge (Fig. 3). Lithic fragments are dominated by quartz grains ranging from 40% to more than 80% (Fig. 7). The major source of quartz close to the Mendeleev Ridge is the Laptev Sea; however, considerable amounts of quartz grains may also originate from portions of the Canadian Archipelago, upstream of the Beaufort Gyre (Bischof et al., 1996). Next in abundance in NP26 cores are carbonate rock fragments, which peak

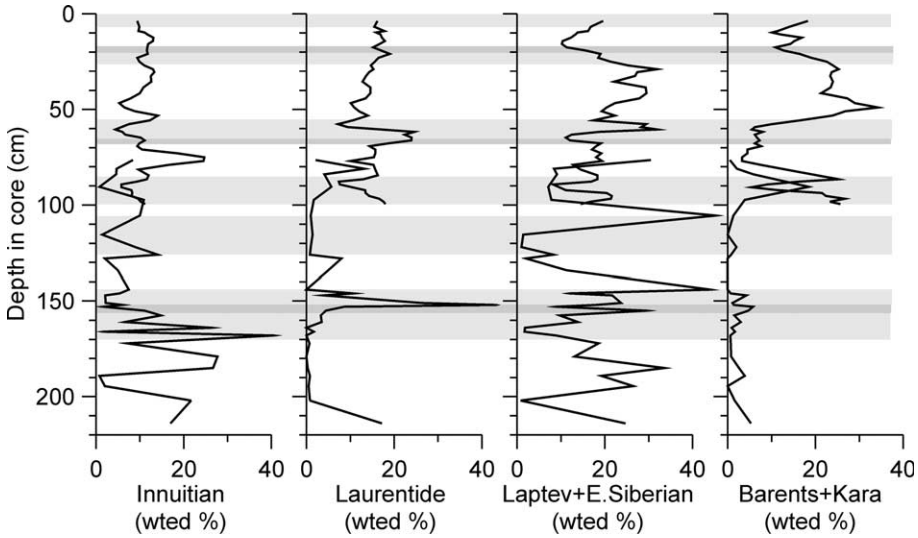

Fig. 8. Iron oxide grain types (weighted %) in NP26 cores (see Fig. 2 for lithology). Fe oxides are matched to source areas after Darby and Bischof (1996).

at the pink-white layers and indicate the Laurentide part of the Canadian Archipelago (Banks and Victoria Islands) as the source area. Remaining clasts are mostly composed of crystalline and clastic sedimentary rocks. The latter fragments, which may be characteristic of the Barents and Kara Sea source or the Mackenzie area of the Canadian Arctic (Bischof et al., 1996), markedly increase in abundance in the upper beds, G2 to B1.

As indicated by the composition of iron oxides, the lower part of the NP26 record is characterized by elevated inputs from the Canadian Archipelago, mostly from its Innuitian part (Queen Elizabeth Islands) (Fig. 8). A distinct spike of Fe oxides from the Laurentide source marks the pink-white carbonate layer between B6 and B7. Elevated concentrations of Laurentide Fe oxides consistently characterize the two other pink-white layers further upcore. Another major source of Fe oxides in the NP26 record is the shelf of the Laptev and East Siberian Seas. Some intervals in the upper part of the record have elevated contents of Fe oxides from the Kara and Barents Seas, consistent with heightened abundances of sedimentary rock fragments.

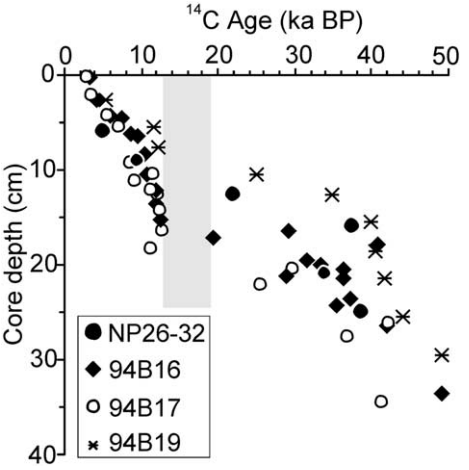

Fig. 9. Age–depth distribution in sediments from the Mendeleev Ridge constructed using data from this study (NP26-32) and USGS 1994 box cores (Fig. 1; Darby et al., 1997; Poore et al., 1999). Reservoir correction applied is −440 yr (Mangerud and Gulliksen, 1975); however, actual reservoir time could be larger in the Arctic Ocean, especially during glacial periods. Shading highlights a possible hiatus between 13 and 19 ka. Note that the age of ~20 ka in 94B16 is an inversion.

5. Discussion

5.1. Age model

Several authors suggest that the apparently cyclic sequence of gray and brown beds in the Arctic Ocean sediments, including cores from the Mendeleev Ridge, reflects a succession of glacial and interglacial/interstadial periods (Belov and Lapina, 1961; Polyak, 1986; Poore et al., 1994; Phillips and Grantz, 1997; Jakobsson et al., 2000). This implies that faunal-rich beds indicate relatively highly productive interglacial environments, significant influence of Atlantic water, and production of well oxygenated bottom waters. In contrast, gray, faunal-poor layers correspond to glacial periods associated with thicker ice cover, suppressed biological production, weaker advection of Atlantic water, and reduced bottom water formation. This interpretation is supported by ^{14}C ages from the upper part of the stratigraphic sequence from several sites across the Arctic Ocean (Fig. 9; Darby et al., 1997; Poore et al., 1999). Although some of these ^{14}C dates, especially in faunal-poor beds, can be biased due to bioturbation and low sediment fluxes, the consistent downcore succession of ages indicates that the two uppermost brown beds (B1 and B2) represent the Holocene and Marine Isotope Stage (MIS) 3, respectively. The intervening gray bed (G1) contains an interval of drastically declined sedimentation rates, possibly including a hiatus, between ca. 13 ka and at least 19 ka. The prevalent age–depth pattern indicates that this episode possibly started as early as 24–25 ka, assuming that the two ^{14}C ages of 19 and 20 ka, inconsistent with the general pattern, might result from contamination by younger material. The non-deposition has been suggested to result from winnowing (Poore et al., 1999). However, the corresponding interval is characterized by very fine, rather than sandy, sediment (Fig. 3; cf. Darby et al., 1997), which points to an exceptionally heavy ice cover during the Last Glacial Maximum (LGM), rather than winnowing, as a cause of non-deposition.

This interpretation is consistent with extremely low abundance or complete absence of biogenic remains during the low-sedimentation interval and immediately above it.

Time control for the Arctic Ocean stratigraphic sequence beyond the range of ^{14}C ages is mostly based on magnetostratigraphy. A distinct decrease in inclination occurring at a same stratigraphic level throughout the Arctic Ocean is largely interpreted as the Brunhes–Matuyama boundary (e.g., Clark et al., 1980; Poore et al., 1993). The succession of brown and gray beds overlying this boundary has been suggested to match the major glacial–interglacial events reflected by the global marine $\delta^{18}O$ scale, MIS 1 to 19 (Fig. 10, central panel; Poore et al., 1993; Phillips and Grantz, 1997; Spielhagen et al., 1997). However, an alternative interpretation of paleomagnetic data from the Lomonosov Ridge suggests that the above decline in inclination is an excursion rather than inversion of magnetic field, which implies a much younger age of sediment and, accordingly, higher

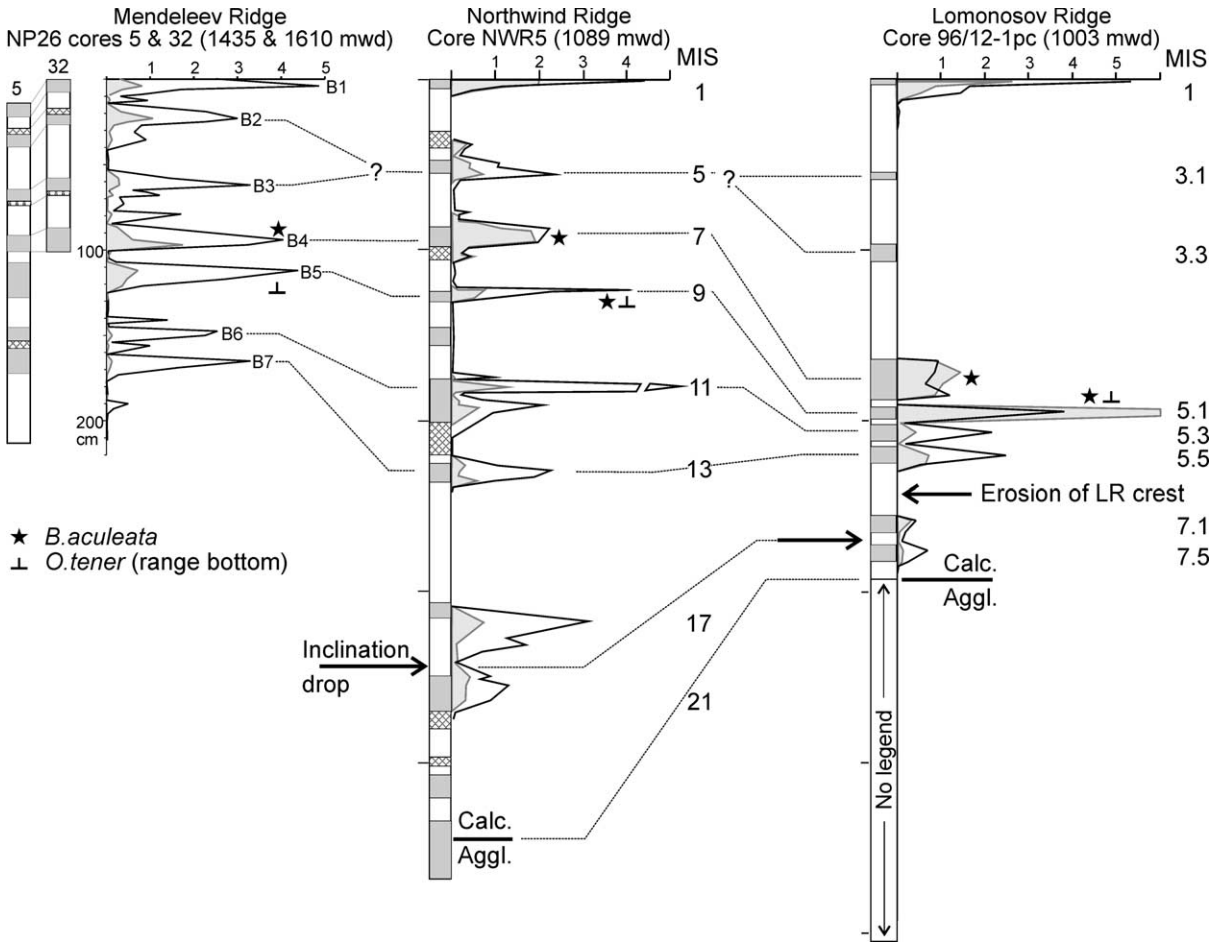

Fig. 10. Correlation of NP26 record with cores from the Northwind Ridge (NWR) (P1-88AR-P5, also referred to as NWR 5; Poore et al., 1993, 1994) and Lomonosov Ridge (LR) (96/12-1pc; Jakobsson et al., 2000, 2001). Interglacial brown mud units are shaded and indexed next to NP26 cores; criss-cross pattern shows pink-white detrital carbonate layers. MIS are shown next to NWR 5 and 96/12-1pc records, as interpreted in respective papers. Curves show numbers of planktonic ($\times 10^3$) and benthic ($\times 10^2$, shaded) >150-μm foraminifers per gram sediment. Arrows left to the NWR and LR cores show a drop in magnetic inclination interpreted as the Brunhes–Matuyama boundary in NWR 5, but not in 96/12-1pc. Also shown are selected biostratigraphic markers, a boundary between agglutinated and calcareous foraminiferal faunas, and a position of glacial erosion on LR.

sedimentation rates (Jakobsson et al., 2000, 2001). This new paleomagnetic approach is coupled with an alternative correlation of glacial–interglacial cycles with the global $\delta^{18}O$ scale, which takes substages into account (Fig. 10, right panel). Independent support for this 'young' age model is provided by the coccolith stratigraphy and by the first application of optically stimulated luminescence dating to the Arctic Ocean sediments (Jakobsson et al., 2001, 2003). We believe that the solution of this stratigraphic dilemma requires refinement of paleomagnetic studies as well as independent chronostratigraphic techniques. In this paper, we show both age models as applied to NP26 cores by correlation with the Northwind ('old') and Lomonosov Ridge ('young') stratigraphies (Fig. 10).

5.2. Stable isotopes

The water $\delta^{18}O$ composition in the Arctic Ocean is primarily controlled by the mixing of isotopically light runoff and marine, Atlantic-derived water with $\delta^{18}O$ composition of near 0‰ (Schlosser et al., 2000 and references therein). Accordingly, both the lateral and vertical distributions of $\delta^{18}O$ in the Arctic Ocean strongly correlate with salinity (Fig. 2). This distribution may be locally modified by the processes of sea ice freezing and melting, which cause the rejection of isotopically light brines during freezing and the release of $\delta^{18}O$-enriched water when ice melts (e.g., Strain and Tan, 1993). The equilibrium calcite (e.c.) $\delta^{18}O$ is additionally affected by temperature that is linked in the Arctic Ocean with the advection of Atlantic-derived water. This results in a lowering of $\delta^{18}O_{e.c.}$ in the Atlantic layer by almost 1‰ in the Eurasia Basin (Bauch et al., 1997; Lubinski et al., 2001), but in the Western Arctic, where the Atlantic influence is weaker, this lowering is much smaller (Fig. 2).

Except for the area near the Fram Strait that is affected by warm Atlantic water, $\delta^{18}O$ values in *Neogloboquadrina pachyderma* (sin.) from surficial bottom sediments throughout the Arctic Ocean generally get lighter towards the Western Arctic (Spielhagen and Erlenkeuser, 1994; Alderman, 1994). This trend is consistent with the increase in runoff component in the surface water, but can also be explained by a change in calcification depth. In the southwestern area of the Eurasia Basin, the bulk of *N. pachyderma* calcifies in the upper part of the intermediate, Atlantic-derived water, whereas in the interior of the Arctic Ocean calcification presumably occurs in the surface/halocline water (Bauch et al., 1997; Volkmann and Mensch, 2001). Core top planktonic $\delta^{18}O$ values from NP26 and adjacent box cores are consistent with this picture: given a *N. pachyderma* (sin.) $\delta^{18}O$ disequilibrium of −1–1.5‰ (Bauch et al., 199; Volkmann and Mensch, 20017), core top values match the local halocline $\delta^{18}O_{e.c.}$ composition of 2–3‰ (Fig. 2). In contrast to planktonic $\delta^{18}O$, not much lateral variation is expected for deep-sea benthic foraminiferal $\delta^{18}O$ in the Arctic Ocean because of generally homogeneous bottom water properties below the Atlantic layer. Our unpublished data confirm this assumption by showing *Cibicidoides wuellerstorfi* $\delta^{18}O$ values in the surficial sediments of mostly 3.5–4‰ without any distinct geographic or bathymetric trend below 1 km water depth.

From the modern distribution of planktonic foraminiferal calcite $\delta^{18}O$ in the Arctic Ocean, we expect that its downcore variations will primarily reflect the history of freshwater budget rather than temperature changes. Indeed, $\delta^{18}O$ fluctuations in the Mendeleev Ridge sediments are generally characterized by heavier values in interglacial/interstadial intervals and light peaks in glacial beds (Fig. 6), in contrast to the global open ocean $\delta^{18}O$ stratigraphy that extends into the Greenland Sea and adjacent area of the Eurasia Basin (e.g., Nørgaard-Pedersen et al., 1998, 2003). The youngest planktonic $\delta^{18}O$ minimum in our record correlates to that in earlier investigated box core records from the Mendeleev Ridge (Poore et al., 1999). This spike is consistently centered at ca. 12 ^{14}C ka and likely represents a major meltwater event corresponding to the last deglaciation of the Arctic margins (termination I). We infer that older $\delta^{18}O$ minima in NP26 cores reflect similar deglacial events. An extended interval of light $\delta^{18}O$ values below B5 presumably indicates a particularly strong flux and storage of meltwater in the Amerasia Basin.

The four maxima (heavy spikes) of planktonic $\delta^{18}O$ reaching $>3.5‰$ (Fig. 6) are ca. 2‰ heavier than modern values in the Mendeleev Ridge area and are as high as the heaviest modern $\delta^{18}O$ values in the Arctic Ocean occurring in fully saline and cold waters near the Fram Strait (Spielhagen and Erlenkeuser, 1994). Because temperatures in surface waters over the Mendeleev Ridge today are just slightly above the freezing point, we infer that heavy $\delta^{18}O$ spikes reflect anomalous reductions in the amount of freshwater in the Amerasia Basin, which caused the shallowing of the halocline and/or the increase in $\delta^{18}O$ composition in surface water. These $\delta^{18}O$ maxima are associated with interglacials and/or interstadials, when significant decrease in riverine fluxes to the Arctic was unlikely. Consequently, we propose that a large portion of the $\delta^{18}O$ increase was caused by a cessation of low-salinity Pacific surface waters, with a $\delta^{18}O$ value ca. $-1.5‰$ lower than Atlantic waters, when the Bering Strait was closed. The present sill depth is 40–50 m, but it may have been even shallower in the past. Brown beds with lower $\delta^{18}O$ values, notably B1, B4, and B6–7, would then correspond to the highest sea level stands, such as during the Holocene and MIS 5.1 and 5.5 (e.g., Lambeck and Chappell, 2001).

The general consistency of changes in planktonic and benthic $\delta^{18}O$ downcore records, although with different amplitudes, suggests the existence of a mechanism of transmitting the $\delta^{18}O$ signal from surface to bottom waters in the Arctic Ocean. In the modern circulation system, such downwelling is provided by the descent of brines released in the process of ice freezing over the Arctic shelves. Another potential mechanism during glaciations could be by supercooling of surface water, including glacial meltwater, beneath an ice shelf (Foldvik and Gammelsrød, 1988). Light excursions of 1‰ in *Cibicidoides wuellerstorfi* $\delta^{18}O$ co-occur with light planktonic $\delta^{18}O$ values within G2 and at the bottom of B7; another light benthic $\delta^{18}O$ event is revealed in *Oridorsalis tener* in the upper part of G3. Similar excursions in glacial and deglacial sediments from the Norwegian-Greenland Sea have been interpreted as an intense downmixing of isotopically light surficial water by ice freezing or supercooling processes (Vogelsang, 1990; Vidal et al., 1998; Dokken and Jansen, 1999; Bauch and Bauch, 2001).

The values of $\delta^{13}C$ in *Neogloboquadrina pachyderma* (sin.) in surficial sediments increase from the Fram Strait towards the Amerasia Basin despite an increase in ice coverage (Spielhagen and Erlenkeuser, 1994). This pattern may be explained by a shift in habitats of *N. pachyderma* to surface/halocline waters, because the shelf-born halocline water is ventilated better than the Atlantic-derived water (e.g., Anderson et al., 1999). Organic productivity does not appear to affect significantly the planktonic $\delta^{13}C$ in the Arctic Ocean (Bauch et al., 2000). It is reasonable to assume that high interglacial planktonic $\delta^{13}C$ values (Fig. 6) reflect the import of surface and halocline water from well-ventilated shelves, such as occurs today (cf. Bauch et al., 2000). In addition cold temperatures and enhanced air–sea exchange of CO_2 would have caused elevated $\delta^{13}C$ in surface water ΣCO_2 (Charles et al., 1993). In contrast, during glacial periods with low sea levels and ice sheet growth, fluxes of water from the shelves to the Arctic Ocean interior were greatly reduced, which resulted in low $\delta^{13}C$ values. This lowering was possibly enhanced by a more solid ice cover and reduced air–sea exchange of CO_2.

The general co-variation of downcore changes in planktonic $\delta^{13}C$ and $\delta^{18}O$ indicates the possibility of a common control. This control could be the restriction of Arctic circulation during glacial periods and the resulting pooling of surface water in the western Arctic Ocean (cf. Poore et al., 1999; Nørgaard-Pedersen et al., 2003). Such pooling would maintain (1) low $\delta^{18}O$ values by a build-up of runoff and/or meltwater and (2) low $\delta^{13}C$ due to a reduced ventilation.

Downcore values of benthic $\delta^{13}C$ mostly vary consistently with a planktonic record (Fig. 6), indicating that large-scale changes in the Arctic Ocean ventilation similarly affected the surface and deep waters. However, a large offset in *Oridorsalis tener* $\delta^{13}C$ values and a large amplitude of their variations suggest that $\delta^{13}C$ signal in sediment is modified by organic carbon burial rates (cf. Grossman, 1984). The interpretation of the benthic $\delta^{13}C$ signal is complicated by uncertainties

with foraminiferal habitats. It is possible that during 'starvation' periods, infaunal species such as *O. tener* changed their feeding strategy for surface scavenging.

5.3. Benthic paleoecology

The succession of benthic foraminiferal and ostracode assemblages in Mendeleev, Northwind, Alpha, and Lomonosov Ridge sediments indicates significant changes in benthic environments in the deep Arctic Ocean during the Quaternary. These changes could be associated with (1) food supply patterns, controlled by biological productivity and sedimentation, and (2) properties of bottom waters. Recent studies emphasize the significance of productivity/sedimentation conditions for deep-sea benthic meiofauna including foraminifers, especially in oligotrophic areas such as the Arctic Ocean (Wollenburg and Mackensen, 1998; Van der Zwaan et al., 1999 and references therein). On the other hand, the distribution of modern benthic foraminifers and ostracodes in the Arctic Ocean displays a generally good relationship with major bottom water masses (Lagoe, 1979; Polyak, 1990; Ishman and Foley, 1996; Cronin et al., 1994). More studies are needed to understand whether this relationship is merely coincidental or reflects true linkages of the faunal composition with water properties, such as temperature, salinity, and oxygenation.

The arenaceous foraminiferal fauna indicates an ocean-wide dissolution of calcareous tests in the older part of the recovered late Cenozoic stratigraphic sequence (O'Neill, 1981; Scott et al., 1989; Poore et al., 1994; Ishman et al., 1996; Evans and Kaminski, 1998; Jakobsson et al., 2001). The causes for dissolution could include low productivity of calcifying organisms, diminished inputs of high-alkaline surface waters, and enhanced flux of organic carbon (relative to clastic particle flux) to the seafloor (cf. Huber et al., 2000). The latter explanation may be especially important in the context of a 'young' age model for Arctic Ocean sediments discussed above (Jakobsson et al., 2000). This model implies a dramatic increase in sedimentation rates at the top of the arenaceous foraminiferal assemblage zone on the Lomonosov Ridge (Jakobsson et al., 2001). This interpretation is consistent with a change in trace fossil assemblages at the same stratigraphic level on the Northwind Ridge (Phillips and Grantz, 1997), which indicates a change in sedimentation rates and/or organic carbon fluxes. Alternatively, the enhancement of carbonate preservation could be related to the establishment of deep-water convection in the Norwegian-Greenland Sea in the Middle Pleistocene (Henrich et al., 2002). The latter change was time-transgressive, extending west- and northwards across the Norwegian-Greenland Sea between 1.2 and 0.7 Ma, and possibly started affecting the Arctic Ocean even later.

The oldest calcareous benthic foraminiferal assemblages that succeed the arenaceous fauna are characterized by elevated contents of *Bolivina arctica*. Foraminifers with elongated shape, such as *Bolivina*, are generally believed to indicate relatively highly productive infaunal environments (e.g., Corliss and Chen, 1988). In NP26 core 5, *B. arctica* peaks at the bottom of B7, together with the occurrence of *Epistominella exigua* that reaches almost 30% in >100 μm (Fig. 4; cf. Poore et al., 1994). *Epistominella exigua* indicates seasonal high fluxes of phytodetritus to the seafloor (Gooday, 1993; Thomas and Gooday, 1996) and presently lives in the Arctic Ocean only in the seasonally ice-free area adjacent to the Fram Strait. Its presence in B7 implies that the ice margin at that time was located at least seasonally as far north as 80°N in the Amerasia Basin – a marked contrast with present conditions. This interpretation is consistent with a common occurrence of continental shelf foraminifers, mostly *Elphidium* spp., in sediments below B5. These tests are presumably transported into the interior of the Arctic Ocean by drifting ice (Wollenburg, 1995), which requires relatively open-water summer conditions. Elevated content of *Cassidulina teretis* at several intervals below and throughout B4 is suggested to indicate an enhanced advection of Atlantic water into the Arctic Ocean (Lagoe, 1979; Polyak, 1990; Ishman and Foley, 1996), which could be a cause of reduced ice cover.

The switch to *Oridorsalis tener*- and *Stetsonia*

horvathi-dominated assemblages occurred at the bottom of G5 or at the correlative stratigraphic level on the Mendeleev, Northwind, Alpha, and Lomonosov Ridges (Fig. 4; Scott et al., 1989; Poore et al., 1994; Ishman et al., 1996; Jakobsson et al., 2001). *Oridorsalis tener* has been suggested to be adapted to low-nutrition environments (Mackensen et al., 1985), and the distribution of *S. horvathi* appears to be associated with perennial ice cover (Wollenburg and Mackensen, 1998). Therefore, we infer that this ocean-wide change in benthic foraminiferal fauna may signify the decrease in food supply for benthic organisms due to the increase in ice cover of the Arctic Ocean. However, significant changes within the *O. tener*/*S. horvathi* abundance zone show that conditions were not uniformly low-productive. The notable feature for the lower part of this zone is the presence of *Bulimina aculeata*, especially abundant in B4. *Bulimina*, including *B. aculeata* are common for bottom environments with a stable, fairly high flux of organic carbon to the seafloor (Lutze and Coulbourn, 1984; Mackensen et al., 1995). A possible cause for such an environment in the Arctic Ocean could be a drastic reduction of ice cover, however, this scenario is not supported by stable isotope records in B4 that show values similar to those in the Holocene (Fig. 6). Another explanation for increased biological production may be an enhanced input of nutrient-rich Pacific water to the Amerasia Arctic Ocean. Abundant *B. aculeata* may be also associated with oxygen deficiency in interstitial water (e.g., Lutze and Coulbourn, 1984; Hermelin and Shimmield, 1990). It is noteworthy that the correlative interval with *B. aculeata* in the Lomonosov Ridge record has a specific olive-gray color (Jakobsson et al., 2001), possibly indicating a more reduced geochemical environment than during other interglacials.

Several more stratigraphic intervals have characteristic foraminiferal compositions including accessory species that do not live in the modern Arctic Ocean, such as *Alabaminella weddellensis* (G4), *Gyroidinoides lamarckianus* (B 5–7), *Gyroidinoides orbicularis* (B2–upper G2), and *Nuttalides umboniferus* (G2–G3). We believe that occurrences of these species, although in minor proportions, indicate unique hydrography and/or productivity regimes in the development of the Arctic Ocean. The modern-type benthic foraminiferal fauna characterized by relatively high abundances of *Eponides tumidulus horvathi*, *Quinqueloculina akneriana*, and *Valvulineria arctica* formed during the deposition of B2, that is, during MIS 3.

5.4. Paleocirculation and glacial history

The abundance of iron oxide grains from the Laptev and East-Siberian Seas throughout the NP26 record may indicate the importance of sea ice for the net transportation of sediment to the Mendeleev Ridge (cf. Bischof and Darby, 1997). However, the pulsed nature of the IRD abundance and the variability of its composition mostly reflect the history of iceberg discharge related to the build-up and disintegration of ice sheets on the Arctic Ocean periphery.

The composition of Fe oxide grains in the lower part of the NP26 record, below G5, has a strong Canadian Archipelago signature (Fig. 8). The interval below or including G5 is also characterized by generally light $\delta^{13}C$ and $\delta^{18}O$ values, presumably indicating restricted circulation and the pooling of freshwater in the Amerasia Basin. Associated benthic assemblages are interpreted to indicate reduced summer ice cover and enhanced inflow of Atlantic water during interglacials. In a maximal age model, this lower interval (G5 and below) is tentatively correlated to MIS 16–12, yet in a 'young' model, it corresponds only to MIS 6 to 5b or 5d (Fig. 10). Regardless of an absolute age, the lowermost gray unit G6 correlates to the top of an interval in Lomonosov Ridge sediments associated with the erosion of the ridge crest to a water depth of 1 km by an ice shelf that extended from the Barents Sea (Jakobsson, 1999; Polyak et al., 2001; Jakobsson et al., 2001). Bedforms on the Chukchi Borderland extending to 700 m depth also evidence the grounding of an ice shelf, potentially of the same age, that advanced from the Alaskan/Canadian margin (Polyak et al., 2001). This paleogeographic situation suggests a very large ice sheet in North America, which should have reduced the water export from the Arctic Ocean. This, together with meltwater inputs

from the ice sheet, likely resulted in the pooling of large amounts of freshwater in the Amerasia Basin, as reflected in a prolonged period of low $\delta^{13}C$ and $\delta^{18}O$ values. However, the conditions during this period were not uniform and included intervals of inferred relatively reduced summer ice cover and high productivity, especially well pronounced in B7.

A noticeable change occurred during the interval between B6 and B5. Stable isotopic records above this transition display regular, high-amplitude fluctuations indicative of alternating glacial and interglacial regimes. Benthic foraminiferal assemblages dominated by *Oridorsalis tener* and *Stetsonia horvathi* are generally interpreted to indicate more severe sea ice cover. This condition could be possibly connected with the increased import of the Atlantic water into the Arctic Ocean across the Barents Sea rather than via the Fram Strait, which enhances the cooling of this water (e.g., Schauer et al., 1997). Such a change in the routing of Atlantic water would be caused by a progressive deepening of the Barents Sea shelf by glacial erosion during the Quaternary (Faleide et al., 1996; Rasmussen and Fjeldskaar, 1996). A significant effect of changes in the Barents Sea bathymetry on the passage of Atlantic water to the Arctic has been demonstrated by ocean circulation modeling (Butt et al., 2002) and exemplified by paleoceanographic records from the last deglaciation and the Holocene (Lubinski et al., 2001). Another possible long-term effect of glaciations on the Arctic circulation may have been the deepening of the Canadian Archipelago straits, which facilitates the export of surface water from the Amerasia Basin. Reaching a critical level of this export would cause a shift towards heavier $\delta^{18}O$ values, such as occur on top of G5.

The existence of at least two sets of glacigenic bedforms on the Chukchi Borderland (Polyak et al., 2001) implies several episodes of ice shelf formation over the western Arctic Ocean during glacial maxima. A likely candidate for an extensive ice shelf cover is the penultimate glacial period (G2) that is characterized by a prolonged deposition of very fine, mostly unfossiliferous sediment, bound by sand/IRD spikes (Fig. 3). The central portion of G2 is characterized by a distinct $\delta^{18}O$ minimum in both planktonic and benthic foraminifers (Fig. 6) and is followed by a peculiar benthic fauna that includes *Nuttalides umboniferus*, potentially a low-productivity indicator (Gooday, 1993; Loubere and Fariduddin, 1999). The most recent ice shelf over the Amerasia Basin might have existed during the LGM, as reflected by extremely low sedimentation rates and almost complete absence of biogenic remains during the interval of 13 to at least 19 ka (Figs. 3 and 9). A pronounced $\delta^{13}C$ and $\delta^{18}O$ minimum at ca. 12 ka emphasizes the dramatic effect of the last deglaciation on the Amerasia Basin (cf. Poore et al., 1999).

The disintegration of ice shelves over the Amerasia Basin would have caused surges and outbursts of icebergs into the Arctic Ocean from adjacent ice sheets (cf. Darby et al., 2002). The magnitude of such events is exemplified by a discharge of estimated 80 000 km^3 from just one ice stream at the northern Laurentide margin shortly before 10 ka (Clark and Stokes, 2001) and up to 10^6 km^3 ice reaching Fram Strait from this ice sheet over 1–2 kyr (Darby et al., 2002). We expect such discharges to be reflected in sedimentary records by distinct IRD spikes exemplified by pink-white carbonate layers indicative of material from the Laurentide part of the Canadian Archipelago (cf. Bischof et al., 1996; Darby et al., 2002). Three pronounced discharge events from this area are recorded in NP26 cores by detrital carbonate layers and Laurentide iron oxide grains (Figs. 3, 7 and 8). The ~10-ka ice stream event is not clearly expressed here, possibly due to insufficient resolution, but forms a distinct spike in cores from the Chukchi Rise (J. Bischof, personal communication, 2000). The increase in IRD inputs from the Barents and Kara Seas in the youngest part of the NP26 record probably indicates the expansion of ice sheets in that sector of the Arctic shelf in the latest Pleistocene.

6. Summary and conclusions

The combined paleontological, stable isotopic, and IRD provenance data from NP26 sediment cores provide new insights into the Quaternary

paleoceanographic evolution of the Arctic Ocean, despite the age model uncertainty. The most evident feature of the investigated sedimentary record is the cyclic alternation of glacial and interglacial regimes, expressed in lithology and paleontological and stable isotopic compositions, consistent with results from other areas in the central Arctic Ocean with similar sedimentation rates (Phillips et al., 1992; Poore et al., 1993, 1994; Phillips and Grantz, 1997; Jakobsson et al., 2000). Fluctuations in $\delta^{13}C$ and $\delta^{18}O$ records acquired regularity and highest amplitudes after the glacial interval G5; the onset of this interval also marks noticeable changes in benthic assemblages and in mineral grain composition. We suggest that these changes indicate a transition from the environment characterized by a large freshwater component in surface waters and a somewhat reduced summer sea ice cover to more stable perennial ice and periodically lessened freshwater amounts. Although the causes of this transition are unclear, we hypothesize that they were possibly associated with large-scale glaciations at the Arctic Ocean periphery. Glacial erosion has deepened the Barents Sea shelf, which opened a route for importing Atlantic water colder than that entering via the Fram Strait. In a similar way, the deepening of the Canadian Archipelago straits could intensify the drainage of surface waters from the Amerasia Basin during interglacials. We note that further back in time the Arctic Ocean had experienced another pronounced change in hydrographic and/or sedimentation regime, as expressed in the establishment of conditions favorable for preservation of carbonates (O'Neill, 1981; Scott et al., 1989; Poore et al., 1994; Evans and Kaminski, 1998; Jakobsson et al., 2001).

Pronounced fluctuations in foraminiferal calcite $\delta^{18}O$ and $\delta^{13}C$ in the upper portion of the record from the Mendeleev Ridge depict profound changes in freshwater balance and/or ventilation rates of the Arctic Ocean. Lighter stable isotopic values indicate higher freshwater inputs and/or residence time, and weaker ventilation of the surface and halocline waters in the Amerasia Basin during glacial periods. The lightest stable isotopic spikes characterize deglacial events such as the last deglaciation at ca. 12 kyr BP (cf. Poore et al., 1999). Intervals with anomalously heavy $\delta^{18}O$ values were possibly related to interstadial periods with the closed Bering Strait, when the Pacific surface waters with relatively low salinity and $\delta^{18}O$ composition ceased to enter the Arctic Ocean.

Extremely low numbers or complete absence of biogenic remains in sediments from some glacial intervals support the notion that the western Arctic Ocean was possibly covered by very thick pack ice or extensive ice shelves during Pleistocene glaciations (e.g., Grosswald and Hughes, 1999; Nørgaard-Pedersen et al., 2003). The lowermost lithological unit recovered by NP26 cores (G6) correlates to the unit deposited during and/or immediately after the inferred ice shelf erosion on Lomonosov Ridge, constrained by different age models to some time between MIS 6 and 16 (Jakobsson et al., 2001). Younger ice shelves over the Amerasia Basin may have existed during the penultimate and, possibly, the last glaciation. The latter would have advanced at 19 ka or somewhat earlier and disintegrated at ca. 13 ka, followed by a pronounced meltwater event indicated by stable isotopic data. We infer that ice shelf collapses caused dramatic discharges of ice into the Arctic Ocean from the North American ice sheets (e.g., Clark and Stokes, 2001; Darby et al., 2002); such events originating from the Laurentide part of the Canadian Archipelago are presumably marked in sedimentary records by detrital carbonate layers and iron oxide grains from Banks and Victoria Islands.

Some stratigraphic intervals of the Mendeleev Ridge record have unique paleontologic signatures that have no analogs in the modern Arctic Ocean. The most evident indicator of a non-analogous paleoceanographic situation is a benthic foraminiferal assemblage with abundant *Bulimina aculeata* centered in interglacial unit B4; this assemblage zone occurs throughout the Amerasia Basin, including the Lomonosov Ridge (Poore et al., 1994; Ishman et al., 1996; Jakobsson et al., 2001). We infer that the *B. aculeata* assemblage reflects enhanced biological productivity, possibly connected with elevated inflow of Pacific water, and/or reduced oxygenation of bottom water.

We note that our understanding of the Quaternary history of the Arctic Ocean is restrained by the uncertainties with age models beyond the range of ^{14}C dating. By means of bio- and lithostratigraphy, we correlate the Mendeleev Ridge record with those from other areas of the Arctic Ocean, such as the Northwind and Lomonosov Ridges (Fig. 10), but we are cautious to make a definitive judgement regarding an age model for these sediments. Because age model choice strongly affects the interpretation of paleoceanographic evolution, this uncertainty prompts an urgency in refining and verifying the chronostratigraphy for the Arctic Ocean sediments.

Acknowledgements

This work was partially supported by the USA NSF awards OPP-9614451, 9817051, and 9817054. We are grateful to Ye.V. Telepnev and I.A. Alekseev, who collected the cores, and to all people who assisted with sample processing and analytical efforts at various stages of this work. This is Byrd Polar Research Center Publication No. C-1281 and Woods Hole Oceanographic Institution Contribution No. 11002.

References

Aagard, K., Swift, J.H., Carmack, E.C., 1985. Thermohaline circulation in the arctic mediterranean seas. J. Geophys. Res. 90, 4833–4846.

Aagard, K., Darby, D., Falkner, K., Flato, G., Grebmeier, J., Measures, C., Walsh, J., 1999. Marine Science in the Arctic: A Strategy. Arctic Research Consortium of the United States (ARCUS), Fairbanks, AK, 84 pp.

Alderman, S.E., 1994. Correlation of Coretop $\delta^{18}O$ and Modern Salinity Gradients in the Arctic Ocean. M.S. Thesis, MIT-WHOI, Woods Hole, MA.

Anderson, L.G., Jones, E.P., Rudels, B., 1999. Ventilation of the Arctic Ocean estimated by a plume entrainment model constrained by CFCs. J. Geophys. Res. 104, 13423–13429.

Bauch, D., Carstens, J., Wefer, G., 1997. Oxygen isotope composition of living *Neogloboquadrina pachyderma* (sin.) in the Arctic Ocean. Eart Planet. Sci. Lett. 146, 47–58.

Bauch, D., Carstens, J., Wefer, G., Thiede, J., 2000. The imprint of anthropogenic CO_2 in the Arctic Ocean: evidence from planktic $\delta^{13}C$ data from watercolumn and sediment surfaces. Deep-Sea Res. II 47, 1791–1808.

Bauch, D., Bauch, H., 2001. Last glacial benthic foraminiferal $\delta^{18}O$ anomalies in the polar North Atlantic: a modern analogue evaluation. J. Geophys. Res. 106 (C5), 9135–9143.

Belov, N.A., Lapina, N.N., 1961. Donnye otlozheniya Arkticheskogo bassejna (Seafloor sediments of the Arctic Basin). Morskoj Transport, Leningrad, 150 pp. (in Russian).

Belyaeva, N.V., Khusid, T.A., 1990. Distribution patterns of calcareous foraminifers in Arctic Ocean sediments. In: Bleil, U., Thiede, J. (Eds.), Geological History of the Polar Oceans: Arctic versus Antarctic. NATO ASI Ser. C 308, 311–316.

Bischof, J.F., Darby, D.A., 1997. Mid- to Late Pleistocene ice drift in the Western Arctic Ocean: evidence for a different circulation in the past. Science 277, 74–78.

Bischof, J.F., Clark, D.L., Vincent, J.-S., 1996. Pleistocene paleoceanography of the central Arctic Ocean: The sources of ice rafted debris and the compressed sedimentary record. Paleoceanography 11, 743–756.

Butt, F.A., Drange, H., Elverhøi, A., Ottera, O.H., Solheim, A., 2002. Modelling Late Cenozoic isostatic elevation changes in the Barents Sea and their implications for oceanic and climatic regimes: preliminary results. Quat. Sci. Rev. 21, 1643–1660.

Carmack, E.C., Aagard, K., Swift, J.H., Macdonald, R.W., McLaughlin, F.A., Jones, E.P., Perkin, R.G., Smith, J.N., Ellis, K., Kilius, L., 1997. Changes in temperature and contaminant distributions within the Arctic Ocean. Deep-Sea Res. II 44, 1487–1502.

Charles, C.D., Wright, J.D., Fairbanks, R.G., 1993. Thermodynamic influences on the marine carbon isotope record. Paleoceanography 8, 691–697.

Clark, C.D., Stokes, C.R., 2001. Extent and basal characteristics of the M'Clintock Channel ice stream. Quat. Int. 86, 81–101.

Clark, D.L., Whitman, R.R., Morgan, K.A., Mackey, S.D., 1980. Stratigraphy and glacial-marine sediments of the Amerasian Basin, central Arctic Ocean. Geol. Soc. Am. Spec. Pap. 181, 57 pp.

Clough, L.M., Ambrose, W.G., Jr., Cochran, K.J., Barnes, C., Renaud, P.E., Aller, R.V., 1997. Infaunal density, biomass and bioturbation in the sediments of the Arctic Ocean. Deep-Sea Res. II 44, 1683–1704.

Corliss, B.H., Chen, C., 1988. Morphotype patterns of Norwegian Sea deep-sea benthic foraminifera and ecological implications. Geology 16, 716–719.

Cranston, R.E., 1997. Organic carbon burial rates across the Arctic Ocean from the 1994 Arctic Ocean Section expedition. Deep-Sea Res. II 44, 1705–1724.

Cronin, T.M., Holtz, T.R., Stein, R., Spielhagen, R., Fütterer, D., Wollenburg, J., 1995. Late Quaternary paleoceanography of the Eurasian Basin. Arctic Ocean. Paleoceanogr. 10, 259–281.

Cronin, T.M., Holtz, T.R., Jr., Whatley, R.C., 1994. Quaternary paleoceanography of the deep Arctic Ocean based on quantitative analysis of Ostracoda. Mar. Geol. 119, 305–332.

Danilov, I.D., Telepnev, Ye.V., Chugunov, A.B., Belyaeva, N.V., Khusid, T.A., Virina, Ye.I., Polyakova, Ye.I., 1991.

Paleogeographic investigation of bottom sediments of the central Arctic Ocean (Mendeleyev Ridge) (translated from Russian). Oceanology (USSR) 31, 77–82.

Darby, D.A., 2003, Sources of sediment found in sea ice from the western Arctic Ocean, new insights into processes of entrainment and drift patterns. J. Geophys. Res. 108, 13-1 to 13-10.

Darby, D.A., Bischof, J.F., 1996. A statistical approach to source determination of lithic and Fe-oxide grains: an example from the Alpha Ridge, Arctic Ocean. J. Sediment. Res. 66, 599–607.

Darby, D.A., Bischof, J.F., Jones, G.A., 1997. Radiocarbon chronology of depositional regimes in the western Arctic Ocean. Deep-Sea Res. II 44, 1745–1757.

Darby, D.A., Bischof, J.F., Spielhagen, R.F., Marshall, S.A., Herman, S.W., 2002. Arctic ice export events and their potential impact on global climate during the late Pleistocene. Paleoceanogr. 15-1 to 15-17.

Delworth, T.L.S., Manabe, S., Stouffer, R.J., 1997. Multidecadal climate variability in the Greenland Sea and surrounding regions: a coupled simulation. Geophys. Res. Lett. 24, 257–260.

Dokken, T., Jansen, E., 1999. Rapid changes in the mechanism of ocean convection during the last glacial period. Nature 401, 458–461.

Ekwurzel, B., Schlosser, P., Mortlock, R.A., Fairbanks, R.G., Swift, J.H., 2001. River runoff, sea ice meltwater and Pacific water distribution and mean residence times in the Arctic Ocean. J. Geophys. Res. 106, 9075–9092.

Evans, J.R., Kaminski, M.A., 1998. Pliocene and Pleistocene chronostratigraphy and paleoenvironment of the central Arctic Ocean, using deep water agglutinated foraminifera. Micropaleontology 44, 109–130.

Faleide, J.I., Solheim, A., Hjelstuen, B.O., Andersen, E.S., Vanneste, K., 1996. Late Cenozoic evolution of the western Barents Sea-Svalbard continental margin. Global Planet. Change 12, 53–74.

Foldvik, A., Gammelsrød, T., 1988. Notes on Southern Ocean hydrography, sea-ice and bottom-water formation. Palaeogeogr. Palaeoclimatol. Palaeoecol. 67, 3–17.

Gooday, A.J., 1993. Deep-sea benthic foraminiferal species which exploit phytodetritus: characteristic features and controls on distribution. Mar. Micropaleontol. 22, 129–146.

Gosselin, M., Levasseur, M., Wheeler, P.A., Horner, R.A., Booth, B.C., 1997. New measurements of phytoplankton and ice algal production in the Arctic Ocean. Deep-Sea Res. II 44, 1623–1644.

Grossman, E.L., 1984. Stable isotope fractionation in live benthic foraminifera from the southern California borderland. Palaeogeogr. Palaeoclimatol. Palaeoecol. 47, 301–327.

Grosswald, M.G., Hughes, T.J., 1999. The case for an ice shelf in the Pleistocene Arctic Ocean. Polar Geogr. 23, 23–54.

Henrich, R., Baumann, K.-H., Huber, R., Meggers, H., 2002. Carbonate preservation records of the past 3 Myr in the Norwegian-Greenland Sea and the northern North Atlantic: implications for the history of NADW production. Mar. Geol. 184, 17–39.

Hermelin, J.O.R., Shimmield, B.G., 1990. The importance of the oxygen minimum zone and sediment geochemistry in the distribution of recent benthic foraminifera in the Northwest Indian Ocean. Mar. Geol. 91, 1–29.

Huber, R., Meggers, H., Baumann, K.-H., Henrich, R., 2000. Recent and Pleistocene carbonate dissolution in sediments of the Norwegian-Greenland Sea. Mar. Geol. 165, 123–136.

Huh, C.A., Pisias, N.G., Kelley, J.M., Maiti, T.C., Grantz, A., 1997. Natural radionuclides and plutonium in sediments from the Western Arctic Ocean: sedimentation rates and pathways of radionuclides. Deep-Sea Res. II 44, 1725–1744.

Ishman, S.E., Foley, K.M., 1996. Modern benthic foraminifer distribution in the Amerasian Basin, Arctic Ocean. Micropaleontology 42, 206–220.

Ishman, S.E., Polyak, L., Poore, R.Z., 1996. An expanded record of Pleistocene deep Arctic change: Canada Basin, western Arctic Ocean. Geology 24, 139–142.

Jakobsson, M., 1999. First high-resolution chirp sonar profiles from the central Arctic Ocean reveal erosion of Lomonosov Ridge sediments. Mar. Geol. 158, 111–123.

Jakobsson, M., Løvlie, R., Al-Hanbali, H., Arnold, E., Backman, J., Mörth, M., 2000. Manganese/color cycles in Arctic Ocean sediments constrain Pleistocene chronology. Geology 28, 23–26.

Jakobsson, M., Løvlie, R., Arnold, E., Backman, J., Polyak, L., Knutsen, J.O., Musatov, E., 2001. Pleistocene stratigraphy and paleoenvironmental variation from Lomonosov Ridge sediments, central Arctic Ocean. Global Planet. Change 31, 1–21.

Jakobsson, M., Backman, J., Murray, A., Løvlie, R., 2003. Optically stimulated luminescence dating supports central Arctic Ocean cm-scale sedimentation rates. Geochem. Geophys. Geosyst. 2.

Jones, E.P., Anderson, L.G., Swift, J.H., 1998. Distribution of Atlantic and Pacific waters in the upper Arctic Ocean: implications for circulation. Geophys. Res. Lett. 25, 765–768.

Jones, R.L., Whatley, R.C., Cronin, T.M., Dowsett, H.J., 1999. Reconstructing late Quaternary deep-water masses in the eastern Arctic Ocean using benthonic Ostracoda. Mar. Micropaleontol. 37, 251–272.

Lagoe, M.B., 1979. Recent benthonic foraminiferal biofacies in the Arctic Ocean. Micropaleontology 25, 214–224.

Lambeck, K., Chapell, J., 2001. Sea level change through the last glacial cycle. Science 292, 679–686.

Loubere, P., Fariduddin, M., 1999. Quantitative estimation of global patterns of surface ocean biological productivity and its seasonal variation on timescales from centuries to millennia. Global Biogeochem. Cycles 13, 115–133.

Lubinski, D.A., Polyak, L., Forman, S.L., 2001. Deciphering the Latest Pleistocene and Holocene inflows of freshwater and Atlantic water to the deep northern Barents and Kara seas: Foraminifera and stable isotopes. Quat. Sci. Rev. 20, 1851–1879.

Lutze, G.F., Coulbourn, W.T., 1984. Recent benthic foraminifera from the continental margin of northwest Africa: community structure and distribution. Mar. Micropaleontol. 8, 361–401.

Macdonald, R.W., Carmack, E.C., 1991. Age of Canada Basin deep waters: a way to estimate primary production for the Arctic Ocean. Science 254, 1348–1350.

Mackensen, A., Sejrup, H.P., Jansen, E., 1985. The distribution of living benthic foraminifera on the continental slope and rise off southeast Norway. Mar. Micropaleontol. 9, 275–306.

Mackensen, A., Schmiedl, G., Harloff, J., Giese, M., 1995. Deep-sea foraminifera in the South Atlantic Ocean: ecology and assemblage generation. Micropaleontology 41, 342–358.

Mangerud, J., Gulliksen, S., 1975. Apparent radiocarbon ages of recent marine shells from Norway, Spitsbergen, and Arctic Canada. Quat. Res. 5, 263–273.

Nørgaard-Pedersen, N., Spielhagen, R.F., Thiede, J., Kassens, H., 1998. Central Arctic surface ocean environment during the past 80,000 years. Paleoceanography 13, 193–204.

Nørgaard-Pedersen, N., Spielhagen, R.F., Erlenkeuser, H., Grootes, P.M., Heinemeier, J., Knies, J., 2003. The Arctic Ocean during the Last Glacial Maximum: Atlantic and Polar domains of surface water mass distribution and ice cover. Paleoceanography 18, 8-1 to 8-19.

O'Neill, B.J., 1981. Pliocene and Pleistocene benthic foraminifera from the central Arctic Ocean. J. Paleontol. 55, 1141–1170.

Ostermann, D.R., Curry, W.B., 2000. Calibration of stable isotopic data: An enriched $\delta^{18}O$ standard used for source gas mixing detection and correction. Paleoceanography 15, 353–360.

Perry, R.K., Fleming H.S., 1986. Bathymetry of the Artic Ocean. Geol. Soc. America, Map and Chart Series MC-56.

Phillips, R.L., Grantz, A., 1997. Quaternary history of sea ice and paleoclimate in the Amerasia basin, Arctic Ocean, as recorded in the cyclical strata of Northwind Ridge. Geol. Soc. Am. Bull. 109, 1101–1115.

Phillips, R.L., Grantz, A., Mullen, M.W., Rieck, H.J., McLaughlin, M.W., Selkirk, T.L., 1992. Summary of Lithostratigraphy and Stratigraphic Correlations in Piston Cores from Northwind Ridge, Arctic Ocean, from USCGC Polar Star, 1988. US Geol. Survey Open-file Report 92-426, 114 pp.

Polyak, L.V., 1986. New data on microfauna and stratigraphy of bottom sediments of the Mendeleev Ridge, Arctic Ocean. In: Andreev, S.I. (Ed.), Sedimentogenes i konkrecioobrazovanie v okeane (Sedimentogenesis and nodule-formation in the Ocean). Sevmorgeologia, Leningrad, pp. 40–50 (in Russian).

Polyak, L.V., 1990. General trends of benthic foraminiferal distribution in the Arctic Ocean. In: Kotlyakov, V.M., Sokolov, V.E. (Eds.), Arctic Research: Advances and Prospects. Part 2. Nauka, Moscow, pp. 211–213.

Polyak, L., Edwards, M.H., Coakley, B.J., Jakobsson, M., 2001. Ice shelves in the Pleistocene Arctic Ocean inferred from glaciogenic deep-sea bedforms. Nature 410, 453–457.

Poore, R.Z., Ishman, S.E., Phillips, L., McNeil, D., 1994. Quaternary stratigraphy and paleoceanography of the Canada Basin, western Arctic Ocean. US Geol. Survey Bull. 2080, 32 pp.

Poore, R.Z., Phillips, L., Rieck, H.J., 1993. Paleoclimate record for Northwind Ridge, western Arctic Ocean. Paleoceanography 8, 149–159.

Poore, R.Z., Osterman, L., Curry, W.B., Phillips, R.L., 1999. Late Pleistocene and Holocene meltwater events in the western Arctic Ocean. Geology 27, 759–762.

Rasmussen, E., Fjeldskaar, W., 1996. Quantification of the Pliocene-Pleistocene erosion of the Barents Sea from present-day bathymetry. Global Planet. Change 12, 119–133.

Schauer, U., Muench, R.D., Rudels, B., Timkhov, L., 1997. Impact of eastern Arctic shelf waters on the Nansen Basin intermediate layers. J. Geophys. Res. 102, 3371–3382.

Schlosser, P., Ekwurzel, B., Khatiwala, S., Newton, B., Maslowski, W., Pfirman, S., 2000. Tracer studies of the Arctic freshwater budget. In: Edward, L.L. et al. (Eds.), The Freshwater Budget of the Arctic Ocean. NATO Sci. Ser. 2 70, 453–478.

Scott, D.B., Mudie, P.J., Baki, V., MacKinnon, K.D., Cole, F.E., 1989. Biostratigraphy and late Cenozoic paleoceanography of the Arctic Ocean: foraminiferal, lithostratigraphic, and isotopic evidence. Geol. Soc. Am. Bull. 101, 260–277.

Shackleton, N.J., 1974. Attainment of isotopic equilibrium between ocean water and the benthonic foraminifera genus *Uvigerina*: isotopic changes in the ocean during the last glacial. In: Labeyrie, L. (Ed.), Colloque international sur les méthodes quantitatives d'étude des variation du climat au sours du Pleistocene. Coll. Int. C.N.R.S. 219, 203–209.

Smith, L.M., Miller, G.H., Otto-Bliesner, B., Shin, S., 2002. Sensitivity of the Northern Hemisphere climate system to extreme changes in Holocene Arctic sea ice. Quat. Sci. Rev. 22, 645–658.

Spielhagen, R.F., Erlenkeuser, H., 1994. Stable oxygen and carbon isotopes in planktic foraminifers from Arctic Ocean surface sediments: reflection of the low salinity surface water layer. Mar. Geol. 119, 227–250.

Spielhagen, R.F., Bonani, G., Eisenhauer, A., Frank, M., Frederichs, T., Kassens, H., Kubik, P.W., Mangini, A., Norgaard-Pedersen, N., Nowaczyk, N.R., Schper, S., Stein, R., Thiede, J., Tiedemann, R., Wahsner, M., 1997. Arctic Ocean evidence for late Quaternary initiation of northern Eurasian ice sheets. Geology 25, 783–786.

Steele, M., Boyd, T., 1998. Retreat of the cold halocline layer in the Arctic Ocean. J. Geophys. Res. 103, 10419–10435.

Strain, P.M., Tan, F.C., 1993. Seasonal evolution of oxygen isotope-salinity relationships in high-latitude surface waters. J. Geophys. Res. 98, 14589–14598.

Thomas, E., Gooday, A.J., 1996. Cenozoic deep-sea benthic foraminifera: tracers for changes in oceanic productivity? Geology 24, 355–358.

Van der Zwaan, G.J., Duijnstee, I.A.P., den Dulk, M., Ernst, S.R., Jannink, N.T., Kouwenhoven, T.J., 1999. Benthic foraminifers: proxies or problems? A review of paleoecological concepts. Earth Sci. Rev. 46, 213–236.

Vidal, L., Labeyrie, L., van Weering, T., 1998. Benthic $\delta^{18}O$ records in the North Atlantic over the last glacial period (60–10 kyr): evidence for brine formation. Paleoceanography 13, 245–251.

Vogelsang, E., 1990. Paläo-Ozeanographie des Europäischen Nordmeeres an Hand stabiler Kohlenstoff- und Sauerstoffisotope. Ber. Sonderforsch. 313, Univ. Kiel, 23, 136 pp.

Volkmann, R., Mensch, M., 2001. Stable isotope composition ($\delta^{18}O$, $\delta^{13}C$) of living planktic foraminifers in the outer Laptev Sea and the Fram Strait. Mar. Micropaleontol. 42, 163–188.

Wollenburg, J.E., 1995. Bentische foraminiferenfaunen als wassermassen-, Produktions- und Eisdriftanzeiger in Arktischen Ozean. Ber. Polarforsch. 179, 227 pp.

Wollenburg, J.E., Mackensen, A., 1998. Living benthic foraminifers from the central Arctic Ocean: faunal composition, standing stock and diversity. Mar. Micropaleontol. 34, 153–185.

Yashin, D.S. (Principal Investigator), 1985. Veschestvennyj sostav i geokhimiya donnyh otlozhenij zapadno-arkticheskih morej SSSR (Mineral composition and geochemistry of bottom sediments, Western Arctic seas of the USSR). Technical Report, Sevmorgeologia, Leningrad (in Russian).